Effects of disorder on the electronic structure of undoped polyacetylene

David Vanderbilt

Department of Physics, Center for Materials Science and Engineering, Massachusetts Institute of Technology, Cambridge, Massachusetts 02139

Eugene J. Mele

Xerox Webster Research Center, Webster, New York 14580

(Received 5 May 1980)

A theoretical investigation of disorder in undoped polyacetylene indicates that a substantial amount of topological and structural disorder is consistent with the experimental work done to date. Certain topological defects (chain ends and cross links) are found to be unstable to soliton emission, with the remarkable consequence that odd-membered finite chains always contain a soliton. Relaxations of the stable defects are determined. Various kinds of structural disorder are studied; these include admixtures of *cis*-isomerization, bending and twisting of chains, local interchain interactions, and stochastic bond-length fluctuations. The effect upon the electronic density of states is calculated in each case. When some chain bending is included, that a distribution of interchain interaction and a plausible amount of bond-length disorder may explain the observed broadening of the Peierls edges.

I. INTRODUCTION

The spectacular increase in the conductivity of polyacetylene upon doping[1] has drawn much attention to this material.[2] Partly as a consequence, it is being realized that *undoped* $(CH)_x$ is a fascinating model system in its own right. It is perhaps the simplest system having a strong Peierls distortion, and has been proposed to support domain wall (soliton) excitations between regions of opposite bond alternation.[3,4] Furthermore, it has been suggested that charged solitons may exist in the ground state of lightly doped $(CH)_x$.

Many questions about the undoped material remain controversial or unanswered. Optical absorption and photoconductivity measurements consistently fail to show a sharp edge at the optical absorption threshold characteristic of a 1D (one-dimensional) density of states.[5,6] There is difficulty obtaining a fit between theoretical calculations and the details of the experimental photoemission spectra.[7,8] The explanation of these discrepancies may depend upon gaining an understanding of the structure; the x-ray data in fact suggest a distribution of interchain distances,[9] but little else is known. What is the microscopic fibril structure? What is the typical size of a polymeric unit in the $(CH)_x$ film? Is there significant bending, twisting, splaying, and crosslinking of polymer chains?

While we cannot unambiguously answer such questions, we have investigated theoretically the consequences of various kinds of structural disorder in $(CH)_x$, and find that considerable disorder is consistent with the experimental work done to date. In Sec. II we discuss topological disorder, including chain ends and crosslinks, and discuss solitons and the question of soliton binding to these

sites. In Sec. III we restrict ourselves to infinite chains whose bond alternation remains intact, but consider various kinds of structural disorder which can nevertheless exist. These include regions of cis-$(CH)_x$, bending and twisting of chains, local interactions between chains, and bond-length disorder. Finally, in Sec. IV we present a summary and conclusions, with some speculation about the experimental anomalies mentioned above.

II. TOPOLOGICAL DEFECTS

If it could by synthesized, crystalline trans-$(CH)_x$ would consist of infinite zig-zag chains made up of CH units. The structure is shown in Fig. 1 for a terminated chain, a defect which will be discussed shortly. The system is planar, with each carbon forming sp^2 hybrids in order to bond with its neighbors. There are two filled bonding orbitals per CH unit, and a half filled π band. The theory of the Peierls transition predicts that the system will undergo an asymmetric distortion in order to double the periodicity and open a gap at the Fermi energy,[10] thus explaining (at least qualitatively) the alternation between long (weak) and short (strong) bonds which is sketched in Fig. 1.

By symmetry, the p_z orbitals decouple rigorously from all other orbitals in the system and may be treated independently. This is very useful because it is the π orbitals which control much of the interesting physics of the system, including the optical gap and the possible existence of solitons. The interactions between the π orbitals are shown schematically in Fig. 2(a) for the structure of Fig. 1. A defect of this kind will be designated $1F_w$ because the last π bond connecting to the *one-fold* site is a *weak* bond. (The radical R, which may be H, CH_3, etc., is assumed to have no states
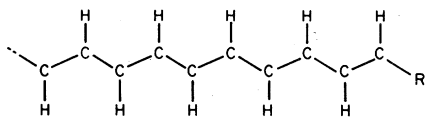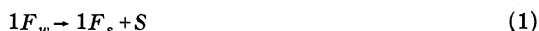

FIG. 1. Structure of a transpolyacetylene chain terminating on a radical R.

of odd-z parity in the neighborhood of the Fermi energy and is therefore ignored.) In Fig. 2(b) we show a chain containing a soliton (S) and terminating on a strong bond ($1F_s$ defect); we will show presently that the reaction

$$1F_w \rightarrow 1F_s + S \qquad (1)$$

is exothermic. This spontaneous emission of a soliton by the $1F_w$ surface configuration has the remarkable consequence that all odd-membered chains must contain a soliton somewhere in their interior.

We now turn to a consideration of the electronic structure of such defects. Before presenting the results of detailed calculations on these structures, we can learn a great deal about the nature of the electronic states, particularly the existence of midgap states, by some powerful general arguments.

All topological defects (chain ends, crosslinks, solitons) can be characterized by a *bond-alternation parity* (BAP) which is defined in the following way. For each semi-infinite chain leaving the defect, sever the chain on a weak bond; then count the atoms remaining in the finite central cluster. If this number is even (odd) the defect has even (odd) BAP. Now if one takes an elementary one-electron Hamiltonian whose zero of energy is at the center of the Peierls gap, it can be shown (see Appendix A) that the density of states is an even function of energy for all such defects, and that as a consequence, all defects of even (odd) BAP have an even (odd) number of localized midgap states. Thus, for example, the $1F_w$ defect and the soliton both have odd BAP, and consequently both have a defect state at mid-
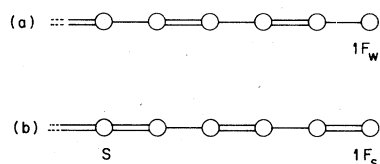
gap. The $1F_s$ defect has even BAP and has no defect states (only midband resonances). Note that BAP is a conserved quantity in reactions such as Eq. (1) above.

The existence of midgap states can be understood intuitively in the limit $|V_s| \gg |V_w|$. In this case one can think of clusters (usually pairs) of atoms connected by strong bonds as "molecules" which then interact slightly with one another via weak bonds. In Fig. 2(a), for example, each strongly bonded pair of sites gives rise to bonding and antibonding molecular orbitals at $\epsilon = \pm V_s$; these are then broadened into bands whose width is on the order of V_w. The last π orbital of the chain has been left out, however, and gives rise to a midgap state at $\epsilon = 0$. In the case of Fig. 2(b), the "triatomic molecule" at the soliton gives rise to an $\epsilon = 0$ midgap state, as well as states at $\epsilon = \pm V_s \sqrt{2}$. A glance at the planar crosslike defects of Fig. 3 indicates that the $3F_{sss}$, $3F_{ssw}$, $3F_{sww}$, and $3F_{www}$ defects will have 2, 1, 0, and 1 midgap states, respectively, these being the number of $\epsilon = 0$ eigenvalues of the corresponding central molecule. (Of course the assumption $|V_s| \gg |V_w|$ is unphysical, but Appendix A makes it clear that the existence of midgap states is symmetry related and remains invariant as long as $|V_s| > |V_w|$.)

It is straightforward to use Green's function techniques to solve for the electronic structure of the defects shown in Figs. 2 and 3. However, this is somewhat pointless because we have no guarantee that any of these defects, in their present form,
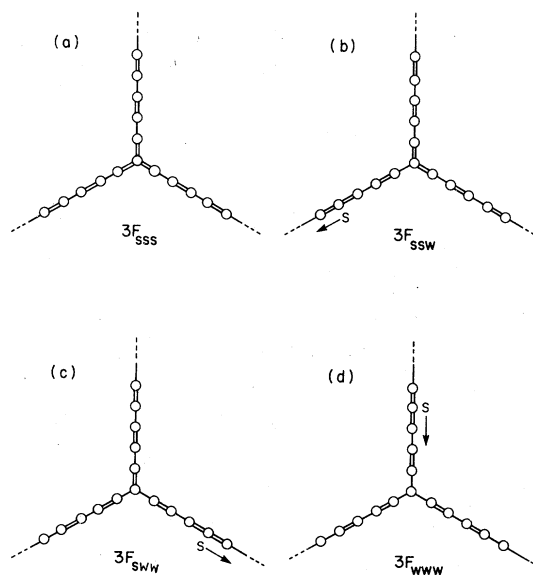

FIG. 2. (a) Schematic interaction diagram for π orbitals of a chain which terminates on a weak π bond ($1F_w$ site). (b) Same for chain containing a soliton (S) and terminating on a strong π bond ($1F_s$ site). The circles represent p_z orbitals, single lines represent weak bonds (interaction v_w), and double lines represent strong bonds (interaction v_s).

FIG. 3. Planar crosslink configurations (a) $3F_{sss}$, (b) $3F_{ssw}$, (c) $3F_{sww}$, (d) $3F_{www}$. Note that the centers interconnect via the reactions $3F_{sss} \rightarrow S + 3F_{ssw}$, $3F_{ssw} \rightarrow S + 3F_{sww}$, and $3F_{sww} + S \rightarrow F_{www}$.

will be stable in the material. Firstly, we expect distortions (relaxations) of the system in the neighborhood of the defects; for example, it is well known from previous theoretical work that the soliton will not remain confined to a pair of strong bonds, as shown in Fig. 2(b), but will spread out over many more sites, creating a region in which the degree of bond alternation is reduced.[4] Secondly, and more drastically, we will show that several of these defects are unstable against the emission of a soliton down one of the chains. Thus our immediate task is to develop a means by which to calculate total energies of various defect configurations, and thereby find stable defects (and their energies) by seraching for total energy minima in configuration space.

Following Su, Schrieffer, and Heeger,[4] we associate to each site n a coordinate u_n for the displacement of the nth CH unit parallel to the chain: the Hamiltonian is then written

$$\mathcal{H} = -\sum_{n,s} v_{n+1,n} C^{\dagger}_{n+1,s} C_{n,s} + \text{H.c.}$$
$$+ \sum_n \tfrac{1}{2} K(u_{n+1} - u_n)^2 - \sum_n \Gamma(u_{n+1} - u_n)$$
$$+ \sum_n \tfrac{1}{2} M \dot{u}_n^2 . \tag{2}$$

Here $v_{n+1,n}$ is the transfer integral, $C_{n,s}$ the annihilation operator for spin s on site n, K the bond-stretch spring constant, and M the CH mass. The Hamiltonian is identical to that of Su, Schrieffer, and Heeger except that the third term has been added to stabilize the chain against contraction due to π bonding. This term has no effect as long as attention is restricted to trial solutions of the infinite chain which do not vary the lattice parameter, but it is important at defect sites because local contractions can and do occur.

In linear order

$$v_{n+1,n} = v_0 - \alpha(u_{n+1} - u_n) \tag{3}$$

so that the static Hamiltonian becomes

$$\bar{\mathcal{H}} = -\sum_{n,s} [(1 + x_n) C^{\dagger}_{n+1,s} C_{n,s} + \text{H.c.}]$$
$$+ \tfrac{1}{2} \sum_n \kappa x_n^2 + \sum_n \gamma x_n , \tag{4}$$

where the renormalizations $\bar{H} = H/v_0$, $x_n = (v_{n+1,n} - v_0)/v_0$, $\kappa = K v_0/\alpha^2$, $\gamma = \Gamma/\alpha$ have been applied to obtain a dimensionless Hamiltonian. For the undimerized chain one has $x_n = x = $ constant and the energy per CH unit is

$$\bar{E} = -(4/\pi)(1 + x) + \tfrac{1}{2}\kappa x^2 + \gamma x , \tag{5}$$

so that to stabilize the chain we choose $\gamma = 4/\pi$. The dimerized chain has $x_n = (-1)^n x$ and

$$\bar{E} = -f(x) + \tfrac{1}{2}\kappa x^2 , \tag{6}$$

where f is obtained by integrating numerically over the density of states. It has the form[11]

$$f(x) = \frac{x^2}{\pi}\left[2\ln\left(\frac{4}{x}\right) - 1\right] + O(x^4). \tag{7}$$

Taking $\partial E/\partial x = 0$ for stability determines

$$\kappa = f'(x)/x . \tag{8}$$

Notice that the couplings κ and γ of Eq. (4) are determined solely by the dimerization parameter x. Thus, within the model, x alone determines the length of solitons (in units of the lattice constant), the relaxations which occur at defects, the relative total energies of various relaxed defects, etc. For completeness we derive estimates for the real spring constant K and coupling α in Appendix B, obtaining results somewhat different from those reported previously. However, this need not concern us at the moment.

We have chosen a π bandwidth of 12 eV ($v_0 = 3$ eV) and Peierls gap of 1.4 eV, which leads to $x = 0.117$ and $\kappa = 3.255$. For each defect configuration, Green's-function techniques are used to determine the local density of states $N_n(\epsilon)$ at each site n. The formalism used is straightforward specialization of the cluster Bethe-lattice method[11,12] to the case of twofold coordination.[12] The contribution of each site to the defect creation energy is, from Eq. (4),

$$\delta\bar{E}_n = \int_{-\infty}^{\epsilon_F} \epsilon N_n(\epsilon) d\epsilon + \tfrac{1}{2}\sum_{n'} (\kappa x_{n'}^2 + \gamma x_{n'}) - \bar{E}_0 , \tag{9}$$

where the sum is over sites which are nearest neighbors to n, and $\bar{E}_0$ is the total energy per site of the uniformly dimerized chain. The sum $\sum_n \delta\bar{E}_n$ converges rapidly and serves to uniquely define the defect total energy. Note that the Hamiltonian of Eq. (4) does not include the changes in σ bonding as one goes to onefold or threefold defects. Therefore, it will only give total energies which are valid for comparing defects of the same coordination. For each defect configuration, the electronic part of Eq. (4) is solved using Green's-function techniques and the lattice energies are simply summed. As a test case we have calculated the ground-state soliton with trial function $u_n = (v_0 x/2\alpha)w_n$ given by

$$w_n = (-1)^n \tanh(n/l) \tag{10a}$$

to have length $l = 9$ and $E = v_0 E = 0.442$ eV, in agreement with Su, Schrieffer, and Heeger.[4]

It now becomes necessary to choose trial functions for the atomic positions in the neighborhood of defects. One wants a trial solution which (i) heals to the normal chain with dimerization x far

from the defect site, (ii) allows for regions of decreased (or increased) dimerization near defects, and (iii) allows the defect site to relax in toward (or out away from) any chain connected to it. We choose

$$w_n = (-1)^n \left(\frac{w_0 + \tanh(n/l)}{1 + w_0 \tanh(n/l)} \right) , \qquad (10b)$$

where the labeling $n = 0, 1, 2, \ldots$ proceeds from the defect site down the chain. The position of the defect site w_0 and decay length l are the two free parameters. Several examples are shown in Fig. 4 [For $|w_0| < 1$ these are truncated solitons since Eq. (10) can be rewritten as $w_n = (-1)^n \tanh(n/l + \tanh^{-1} w_0)$.] We have experimented with other trial solutions, but the essential features are obtained with Eq. (10).

In Figs. 5 and 6 we show the calculated total energies of the $1F_s$ and $1F_w$ defects as a function of w_0 and l. The $1F_s$ defect has an energy minimum at $l = 5$ and $w_0 = 1.75$ with $E = 0.808$ eV. The result $w_0 > 1$ indicates that the final site relaxes in towards the rest of the chain compared to the uniformly dimerized case, and there is a region of increased bond alternation near the defect. The $1F_w$ defect, however, shows a remarkable behavior: no stable configuration exists, but the system wants to relax towards $w_0 = -1$. As can be seen from Fig. 4, this corresponds to the emission of a soliton, leaving behind an unrelaxed $1F_s$ defect. Furthermore, by counting bonds it becomes clear that any finite chain with an odd number of CH units must contain either a $1F_w$ chain end or a soliton; we have shown that the latter is energetically favorable, and thus all odd chains must contain a soliton.

For the three-fold defects of Fig. 3 we used trial solutions with a common l for all three
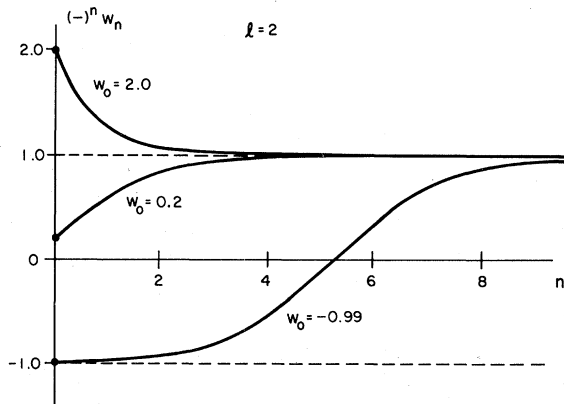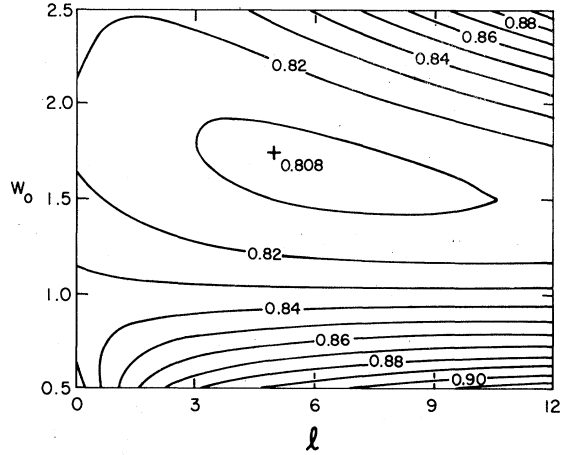
FIG. 5. Total energy in eV of $1F_s$ defect as a function of w_0 and l. The + marks the energy minimum.

chains and different w_0 for different kinds of outgoing chains. We found that the decays $3F_{sss} \to 3F_{ssw} + S$ and $3F_{ssw} \to 3F_{sww} + S$ are exothermic, and that the only stable defects are $3F_{sww}$ ($l = 4$, $w_0^1 = w_0^2 = 1.3$, $w_0^3 = 0.35$, $E = -0.743$ eV) and $3F_{www}$ ($l = 8$, $w_0^1 = w_0^2 = w_0^3 = 0.5$, $E = -0.447$ eV). As in the case of the one-fold defects, the configuration with no midgap state is, not surprisingly, lowest in energy. However, note that $E(3F_{www}) - E(3F_{sww}) < E(\text{soliton})$ so that the $3F_{www}$ is stable and will not decay into $3F_{sww}$ by soliton emission. This contrasts with the situation for one fold defects, where we found that only the $1F_s$ defect was stable. Since the $3F_{www}$ defect has a midgap state, we have the remarkable result that there is a stable three fold defect which is either paramagnetic (if half occupied) or charged (if fully occupied or empty). In the latter case, it is possible that such a defect
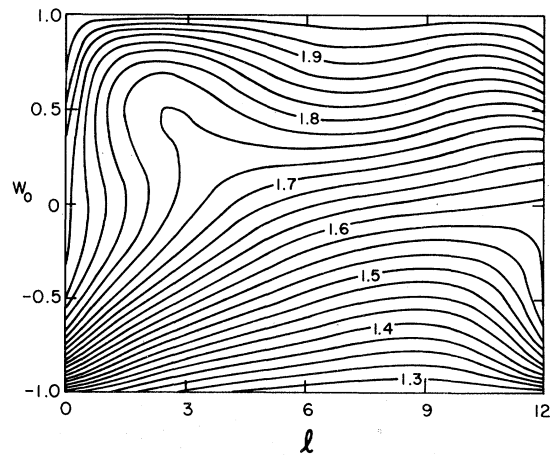
FIG. 4. Trial solutions for the order parameter $(-)^n w_n$ as a function of n, following Eq. (10). In all cases $l = 2$; three choices of w_0 are shown.

FIG. 6. Total energy in eV of $1F_w$ defect as a function of w_0 and l.
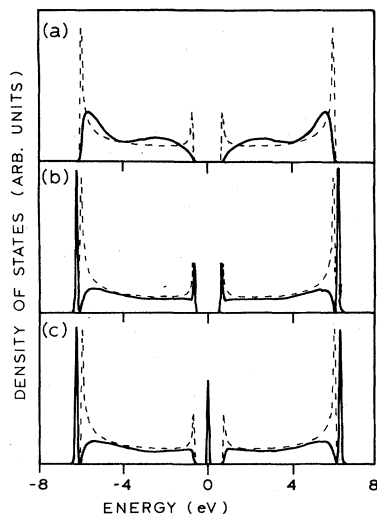
FIG. 7. Calculated densities of states near stable defects (solid curves) and bulk densities of states (dashed curves) for comparison. (a) $1F_s$ defect, (b) $3F_{sww}$ defect, (c) $3F_{www}$ defect.

would show up as a broad ir-active feature at phonon frequencies. Of course, if free solitons are available, the reaction $3F_{www} + S \rightarrow 3F_{sww}$ will purge such defects from the material.

In summary, the stable bond-coordination defects identified to date are the $1F_s$, $3F_{sww}$, and $3F_{www}$ defects. Figure 7 shows the local density of states averaged over a cluster of sites near the defect for each of these three species. Figure 7(a) shows that the $1F_s$ defect causes a considerable shift of weight from the sharp 1D Peierls edges deeper into the bands. This is suggestive in terms of the experimentally observed absence of a sharp optical edge, but the effect has been exaggerated in Fig. 7(a) by averaging the local density of states over a small cluster (four atoms) and consequently a very high density of broken chains would be needed to explain the experimental result. Notice in Fig. 7(b) that the $3F_{sww}$ defect gives rise to shallow trap states 0.06 eV from the Peierls edges, but no deep gap states. Finally for the $3F_{www}$ defect, the formation of the midgap state subtracts a great deal of weight from the Peierls edges [the effect is underestimated by Fig. 7(c) due to averaging the density of states over a small cluster], but any reasonable density of such defects in the pristine material should give rise to noticeable midgap optical absorption (which has not been reported to date). Similar conclusions about the relative stability of the $1F_s$ and $1F_w$ have recently been discussed by Su.[13]

A variety of other topological defects could occur, such as nonplanar crosslinks or benzene-ring chain terminations, but the list of such possibil-

ities is too extensive to pursue here. We prefer to turn our attention at this point to a class of nontopological defects in which we consider only infinite chains with no reversals of bond alternation. There remains considerable variety to be explored in this realm.
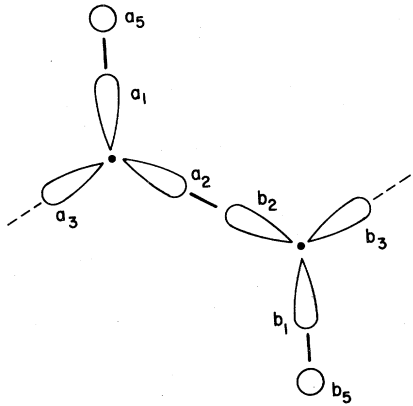
III. STRUCTURAL DISORDER

Even if every polymeric unit in the polyacetylene film were infinite and contained no solitons, there could still be various kinds of disorder present, including regions of cis-$(CH)_x$, bending and twisting of chains, local interactions between touching chains, and variations in amplitude of bond alternation. This disorder could affect the density of states at the Peierls edges or deeper in the valence bands, with consequences for the interpretation of optical and photoemission experiments. We shall consider each of these forms of structural disorder in turn.

In order to do so, we have developed a tight-binding model by fitting to a first-principles calculation on $trans$-$(CH)_x$. The calculation of Karpfen and Petkov[8] was chosen for fitting because its bandwidths appear to agree with photoemission better than other calculations available.[7,14] The resulting tight-binding Hamiltonian is detailed in Table I. Briefly, the basis consists of three sp^2 hybrids, the p_z and the H orbitals in each CH unit. Interactions between all hybrids on nearest neighbors are included.

Figure 8 shows the resulting density of states for $trans$, cis-transoid, and $trans$-cisoid polyacetylene. The p_z orbitals continue to decouple rigorously, so that the region of the Peierls gap is unaffected (assuming the degree of bond alternation is unchanged). However, there are clearly considerable changes deeper in the σ valence bands. If many chains in the film retain regions of cis-isomerization, the resulting density of states would resemble a weighted average of Figs. 8(a)–8(c). However, it was found that such averaging would not materially improve the fit to photoemission by the $trans$-isomer alone.

In Fig. 9 we show what is meant by the terms bend and twist. Both kinds of disorder involve dihedral angle variations only; the sense of the dihedral angle is constant for twist and alternates for bend. ("Splay," or co-planar bending, involves bond angle rather than dihedral angle variations and was therefore dismissed as a less likely possibility.) We have calculated the density of states for structural models with constant bend or twist. These give rise to the circular or helical patterns of Fig. 9 and have the property of being periodic in interaction space. Therefore the

TABLE I. Tight-binding Hamiltonian for $(CH)_x$. Insert shows basis orbitals: a_1, a_2, a_3 are carbon sp^2 hybrids, a_4 (not shown) is p_z, a_5 is a hydrogen s orbital. H_0 gives the form of the on-site part of the Hamiltonian, V gives the nearest-neighbor coupling. θ is the dihedral angle. Parameters are given in the bottom panel.

$$H_0 = \begin{bmatrix} -\epsilon & -\epsilon & -\epsilon & 0 & -V_{CH} \\ -\epsilon & -\epsilon & -\epsilon & 0 & 0 \\ -\epsilon & -\epsilon & -\epsilon & 0 & 0 \\ 0 & 0 & 0 & 0 & 0 \\ -V_{CH} & 0 & 0 & 0 & E_H \end{bmatrix}$$

$$V = \begin{bmatrix} \frac{1}{2}V_\pi\cos\theta & -V_\gamma & -\frac{1}{2}V_\pi\cos\theta & \frac{1}{\sqrt{2}}V_\pi\sin\theta & 0 \\ -V_\gamma & -V_\sigma & -V_\gamma & 0 & 0 \\ -\frac{1}{2}V_\pi\cos\theta & -V_\gamma & \frac{1}{2}V_\pi\cos\theta & -\frac{1}{\sqrt{2}}V_\pi\sin\theta & 0 \\ \frac{1}{\sqrt{2}}V_\pi\cos\theta & 0 & -\frac{1}{\sqrt{2}}V_\pi\sin\theta & -V_\pi\cos\theta & 0 \\ 0 & 0 & 0 & 0 & 0 \end{bmatrix}$$

On site	Strong bond	Weak bond
$\epsilon = 0.65$ eV	$V_\sigma = 18.87$ eV	15.91 eV
$E_H = 8.30$ eV	$V_\pi = 4.45$ eV	3.75 eV
$V_{CH} = 15.65$ eV	$V_\gamma = 3.26$ eV	2.74 eV

FIG. 8. Tight-binding densities of states for crystalline isomers of polyacetylene. (a) $Trans$-$(CH)_x$, (b) cis-transoid $(CH)_x$, (c) $trans$-cisoid $(CH)_x$. Insets show the geometries of each isomer.

cause there are no bonding or antibonding states in that region of the spectrum.

It is quite easy to imagine virtually every chain in the material having some modest amount of bend. We have calculated the density of states for

FIG. 9. Structures resulting from dihedral angle variations may be constructed by folding a strip of paper. Each vertex represents a carbon atom and each heavy line represents a carbon-atom nearest-neighbor C-C bond. A flat strip of paper corresponds to undimerized $trans$-$(CH)_x$. (a) A strongly twisted chain formed by uniform dihedral angle variations of 45°. (b) A strongly bent chain formed by alternating dihedral angle deviations of ±45°.

simplest approach is just to calculate the 1D band structure as a function of the "wace vector" φ which specifies the relative phase of the wave function on neighboring C_2H_2 units. The results are shown in Figs. 10(a) and 10(b). While in principle the bonding and antibonding hybrids could interact strongly with the p_z orbitals, this does not occur for twist at $\varphi = 0$ or for bend at $\varphi = \pi$, because the interactions along the strong and weak bonds are out of phase and almost cancel. For bend the interaction near $\varphi = 0$ is strong and opens a gap near -8 eV where the π band previously crossed a bonding band. For twist near $\varphi = \pi$ manifests itself weakly as an asymmetry in the Peierls edges be-
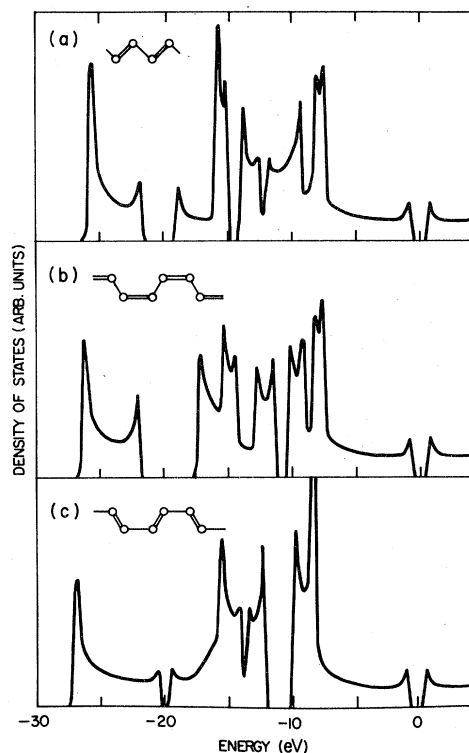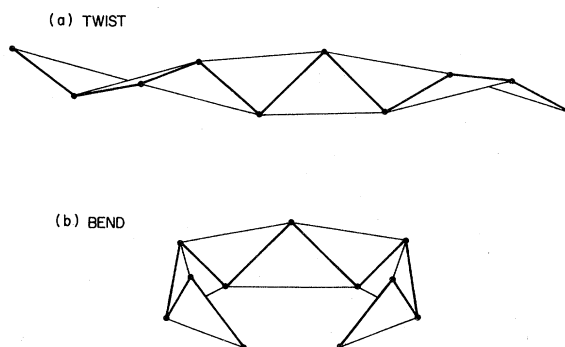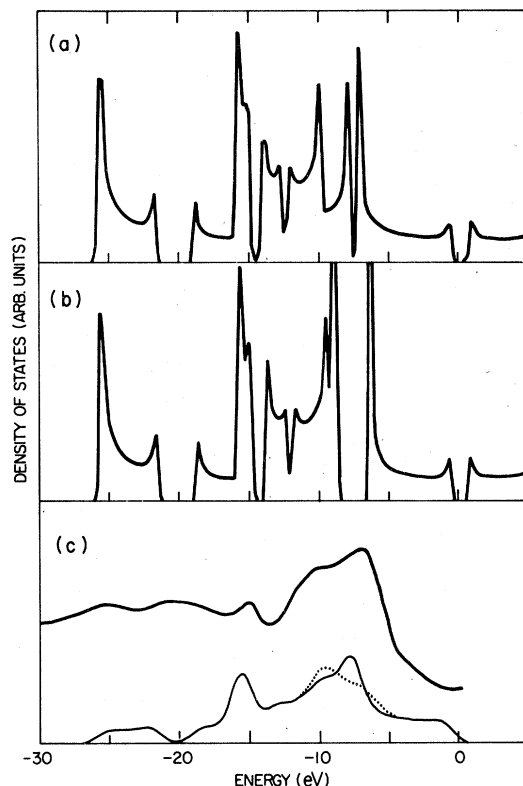
FIG. 10. (a) Tight-binding densities of states for *trans*-(CH)$_x$ with constant twist of 15°. (b) Same for bend of 15°. (c) Light solid line: tight-binding p-state projection of density of states for *trans*-(CH)$_x$ without twist or bend broadened by a 1-eV-wide Gaussian. Dotted line: same for rms bend of 10°. Heavy solid line: experimental photoemission of Ref. 7.

FIG. 11. Density of states in the vicinity of a localized interaction between a pair of crossing (CH)$_x$ chains. Insert gives a schematic interaction diagram; single lines denote v_w, double lines denote v_s, and dotted line denotes w.

different dihedral angles (in 5° increments). Figure 10(c) shows the result of superposing these densities of states according to a Gaussian weighted average with an rms dihedral angle of 10°. Also shown are the density of states without bend and the experimental photoemission of Duke *et al.*[7] Inclusion of some bend allows a modest improvement in the fit to experiment.

In a search for interactions which might show a strong influence on the Peierls region of the spectrum, we have considered the case of local interchain interactions and of bond-strength disorder. The interaction configuration and the resulting density of states for one model of local interchain interactions between crossing chains is shown in Fig. 11, with an exaggerated value of 1.5 eV for the interchain interaction w. The p_z orbitals once again decouple. Because of the presence of odd-fold rings in interaction space, the conclusions of Appendix A are no longer valid, and the density of states is not constrained to be even in energy. We find that an electron trap state has been pulled
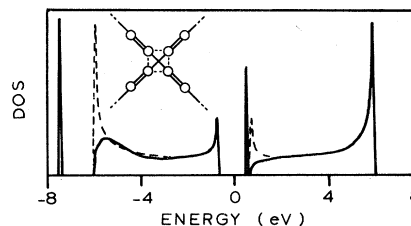
out of the conduction band. A 90° rotation of both chains about their axes induces a similar effect at the valence-band edge. Thus a distribution of interchain interaction along a pair of chains would be expected to induce a slight broadening of the band edges, suppressing the one-dimensional $E^{-1/2}$ singularities at each edge. Such an effect has been described by Grant and Batra[14] who have performed calculations on an idealized three-dimensional model of *cis*-(CH)$_x$. Since there is arguably a distribution of interchain separations in these quasicrystalline samples, this broadening is probably more appropriately described as the band tails of an otherwise unperturbed 1D spectrum than the $\sqrt{E}$3D threshold obtained in Ref. 14. The former interpretation requires that the interchain conductivity occur via hopping between localized tail states.

Finally, we consider the possibility that bond lengths vary randomly away from uniform bond alternation. Bond-length disorder should be considered less probable than stochastic variations in bond angles or interchain separations. However, anticipating that local variations in the packing density of contiguous chains may introduce significant fluctuations in the total crystal potential experienced by the valence electrons, we will consider bond-length fluctuations as well. According to our estimate (see Appendix B) the bond-length change responsible for the gap in crystalline (CH)$_x$ is only ±2.7%, so it is quite easy to imagine that static bond-length disorder of only 1–2% could begin to wash out the gap.

We have tested this idea by constructing a chain segment of 5200 CH units with site positions given by $x_n (-1)^n (1 + s_n)x$, where s_n is chosen independently according to a Gaussian distribution with $\sigma = 0.5$ and zero mean. (For $\sigma = 0$ this would be the perfectly dimerized chain.) Then the bond lengths also follow a Gaussian distribution, with σ' = $(\sigma/\sqrt{2})$ 2.7% or 1% of the bond length. We then connected uniformly dimerized chains to either end of this segment, and averaged the calculated

local density of states over the central 5000 atoms of the segment. Since this is a one-dimensional model, all states are Anderson localized, so that the total density of states is really a sum of δ functions corresponding to each localized state. Therefore, to obtain a smooth average it is necessary to study a segment which is long enough to have many δ functions in every energy interval. Even with 5000 atoms per segment, it was necessary to average the results over four such segments.

The results are shown in Fig. 12. With only a 1% rms bond-length change on each C-C bond, we find a very substantial broadening of the 1D band edges. (Even with $\alpha = 4.1$ eV/Å following Su et al.,[4] a rms deviation gives the same result.) This effect is perhaps better expressed following the arguments presented in Refs. 10 and 15 which treat the electronic spectrum near the Peierls gap in one-dimensional systems in which the lattice distortion becomes uncorrelated over a length ξ. Although in these treatments ξ is envisioned as resulting from thermal disorder, we readily generalize ξ to include static disorder. One obtains a lifetime broadening, Γ, of a "Bloch" state

$$\Gamma = \hbar v_F \xi^{-1}, \tag{11}$$

where v_F is the Fermi velocity in the metallic (undistorted) state. Γ has the effect of "smearing" the electronic spectrum replacing the Peierls gap with a "pseudogap." We estimate $\hbar v_F = 8$ eV Å in $(CH)_x$; consequently a mean coherence length of 40 Å on each chain would be required to explain the observed broadening of the absorption edge, which is not an unreasonably short estimate.

We believe the results described in Figs. 11 and 12 to be the most likely explanation for the absence of a sharp edge in the experiments. Because there is no k-selection rule for a system of localized tail states, this would also explain the observed momentum independence of the absorption edge.[16] Because we have only carried out 1D
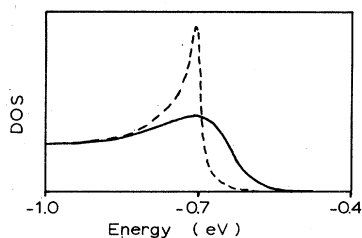

FIG. 12. Solid curve: average density of states near the valence-band edge for a $(CH)_x$ chain with stochastic variations of 1% rms in bond lengths. Dashed curve: crystalline $(CH)_x$ for comparison.

calculations, we have no way of estimating the position of the mobility edge. However, the fact that the disorder in $(CH)_x$ need only be comparable to the bond alternation (which is already small), together with the quasi-1D nature of the system, suggests that this material may be a model system for severe Anderson localization, with an unusually large tail of localized states. Finally, we point out that the degree of broadening of the Peierls edges may be highly sample dependent since the amount of disorder is likely to depend upon preparation conditions. We should note that while the present results suggest mechanisms which broaden the absorption edge, a complete description of the optical spectrum below 2 eV should include a treatment of the excitonic final state.[7] In particular, photoconductivity measurements[6] may be taken as evidence that optical absorption is excitonic within ~1 eV of threshold.

IV. SUMMARY AND CONCLUSIONS

We have studied many different kinds of disorder which can occur in polyacetylene films. The results indicate that moderate structural disorder, including twisting, bending, or local touching of chains, could be virtually universal without having a major impact on the electronic properties of the film. There appears to be a minor improvement in the fit to photoemission when some bend is included. Admixtures of cis-isomerized $(CH)_x$ chains at levels approaching 10% cannot be ruled out by photoemission. Note that Raman[13,15] scattering has been shown to be a more sensitive probe of the cis-trans ratio on $(CH)_x$.

By studying the stability of various possible topological defects to soliton emission and relaxation, we have identified one stable chain termination and two species of stale planar crosslinks. One of the latter has a midgap state, which is not seen in the ir absorption. The other two defects could occur at large densities (on the order of a percent) without having any dramatic effect on the density of states.

Finally, since the bond alternation is already weak, stochastic variations of only 1% in bond length can strongly broaden the 1D Peierls edges. This effect and interactions between randomly packed chains are thought to be the most likely explanations for the observed absence of a sharp edge in some samples.

opportunity to visit the Xerox Webster Research Center where this work was carried out.

APPENDIX A

In this appendix we show that the bond-alternation parity (BAP) as defined in the text specifies whether the system may contain an even or odd number of midgap defect levels. Many of the conclusions we reach are intuitively obvious for specific manageable cases, and we proceed with this analysis to emphasize the generality of these results.

We begin by considering the symmetry of midgap solutions to the one-electron Hamiltonian:

$$\mathcal{H} = \sum_n t_n C_n^\dagger C_{n+1} + \text{H.c.} , \tag{A1}$$

where $t_n = t_1(t_2)$ for odd (even) n. An interaction diagram describing H is given in Fig. 13. Notice that for any eigenfunction of H, φ_λ, with eigenvalue λ, we may construct an eigenfunction $Q\varphi_\lambda$ with eigenvalue $-\lambda$ where

$$Q = \sum_n (-1)^n C_n^\dagger C_n . \tag{A2}$$

At midgap $\lambda \to 0$ and hence φ_0 is an eigenfunction of Q. Inspecting Q, we see that φ_0 must possess nodes on every other site. There are two such functions one may obtain which are labeled (a) and (b) in Fig. 13. For $|t_1| < |t_2|$ the solution (a) [(b)] increases (decreases) as n increases. Subject to the boundary condition that the charge density of such a state in the crystalline dimerized chain possess the translational symmetry of the crystal, we recognize that neither (a) nor (b) are allowed solutions in the crystal, i.e., there are no midgap states in the defect-free chain.

Now consider breaking this chain across a bond. We consider, in turn, breaking the bond $\alpha\beta$ and the bond $\beta\gamma$ shown in Fig. 13. We formally break the bond by continuously reducing the interaction integral along the bond in question to zero. The lower symmetry of the weakened chain permits
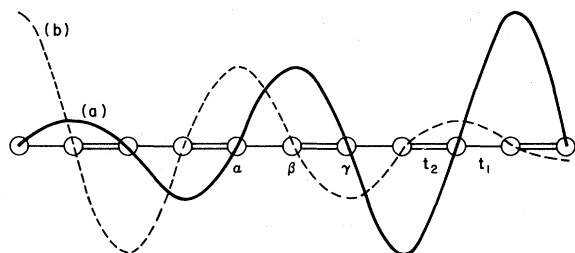

FIG. 13. Dimerized chain with nearest-neighbor interactions t_2 and t_1. Two possible eigenstates of Q are sketched, and described in Appendix A.

midgap solutions which decay to zero at $\pm\infty$. We see that the allowed solution for the chain broken along $\alpha\beta$ would have *zero amplitude* on sites α and β while the solution for the broken $\alpha\beta$ bond may have nonzero amplitude on the terminal sites. In either case the condition $H\varphi_0 = 0$ requires that the defect state has zero amplitude on the next-to-terminal sites. We immediately conclude that the midgap solution for $\delta t_{\alpha\beta}$ is the null solution ($\varphi_0 = 0$), whereas the perturbation $\delta t_{\beta\gamma}$ will produce nonzero solutions which we recognize as surface states on the two severed chains with dangling strong bonds. Thus, breaking a chain along a weak bond will not alter the number of midgap defect levels in the system of interest.

Finally, consider any finite structure to which is attached a set of nonconnected infinite dimerized chains of the type we have considered. We break the appended chains along weak bonds and further require that the finite structure contain no closed odd interaction rings, a requirement which is satisfied by the defects discussed in the text. For such a system it is easy to show that one may always construct a diagonal matrix $\tilde{Q}$, similar to (A2), which has the property

$$\tilde{Q}^\dagger \mathcal{H} \tilde{Q} = -\mathcal{H} . \tag{A3}$$

Hence the density of states is even (for every state at λ there exists a state at $-\lambda$). If the number of sites in the cluster is odd, there must consequently exist an odd number of midgap defect levels in the cluster.

APPENDIX B

In Sec. II, the analysis of Eqs. (2)–(8) was carried out primarily in dimensionless units. Here, we derive estimates for the real spring constant K and electron-phonon coupling α, and compare our results with those of previous authors.

We begin with the experimentally observed[17] Raman-active mode at 1470 cm^{-1} which corresponds to a zone-center optical phonon in which CH units move primarily parallel to the chain axis, with neighboring CH units 180° out of phase.[18] To simplify the analysis we consider the undimerized geometry, and find the screened spring constant K_T is given by $K_T = (\frac{1}{4})M\omega^2 = 25.9$ eV Å^{-2} for $M = 13$ amu. This is related to the unscreened spring constant K of Eq. (2) by

$$K_T = K + K_{\text{scr}} = (\alpha^2/v_0)[\kappa - f''(x)] , \tag{B1}$$

where K_{scr} corresponds to the electronic screening from the first term in the Hamiltonian of Eq. (2). For $x = 0.117$ we find $k = f''(x)/x = 3.255$ and $f'(x) = 2.028$, so that $\alpha^2/v_0 = 21.1$ eV Å^{-2} and $K = 68.6$ eV Å^{-2}. This differs from the estimates of Su, Schrieffer,

and Heeger, who give $\alpha^2/v_0 = 6.8$ eV Å^{-2} and $K/2$ $= 10.5$ eV Å^{-2}.[4]

Taking $v_0 = 3.0$ eV, we find $\alpha = 8.0$ eV Å^{-1}, in agreement with Mele and Rice[19] who give $\alpha = 6.9$ eV Å^{-1}. Then from Eq. (3) we obtain 0.022 Å for the horizontal displacement of the CH units, and 0.038 Å for the bond-length change. Su et al.[4] give $\alpha = 4.1$ eV Å^{-1} and a bond-length change of 0.073 Å. We believe our smaller estimate of the bond-length alternation to be in better agreement with bond-length estimates from other work.[20]

[1]C. K. Chiang, C. R. Fincher, Jr., Y. W. Park, A. J. Heeger, H. Shirikawa, E. J. Louis, S. C. Gau, and A. G. MacDiarmid, Phys. Rev. Lett. 39, 1098 (1977).

[2]Physics Today 32 (9), 19 (1979).

[3]M. J. Rice, Phys. Lett. 71, 4 (1979); 71, 152 (1979).

[4]W. P. Su, J. R. Schrieffer, and A. J. Heeger, Phys. Rev. Lett. 42, 1698 (1979).

[5]C. R. Fincher, Jr., M. Ozaki, M. Tanaka, D. Peebles, L. Lauchlan, A. J. Heeger, and A. G. MacDiarmid, Phys. Rev. B 20, 1589 (1979).

[6]T. Tani, P. M. Grant, W. D. Gill, G. B. Street, and T. C. Clarke, Solid State Commun. 33, 499 (1980); S. Etamad, private communication.

[7]C. B. Duke, A. Paton, W. R. Salaneck, H. R. Thomas, E. W. Plummer, A. J. Heeger, and A. G. MacDiarmid, Chem. Phys. Lett. 59, 146 (1978).

[8]A. Karpfen and J. Petkov, Solid State Commun. 29, 251 (1979).

[9]R. H. Baughman, S. L. Hau, G. P. Pez, and A. J. Signorelli, J. Chem. Phys. 68, 5405 (1978).

[10]P. A. Lee, T. M. Rice, and P. W. Anderson, Phys. Rev. Lett. 31, 462 (1973); M. J. Rice and S. Strassler, Solid State Commun. 13, 125 (1973).

[11]J. D. Joannopoulos and M. L. Cohen, Solid State Phys-ics (Academic, New York, 1971), Vol. 31, p. 71.

[12]D. Vanderbilt and J. D. Joannopoulos, Phys. Rev. B (in press).

[13]W. P. Su, Solid State Commun. (in press); further work concerning stability of bond-alternation defects in $(CH)_x$ is given by B. Horowitz, Solid State Commun. B4, 61 (1980).

[14]P. M. Grant and I. P. Batra, Solid State Commun. 29, 225 (1979).

[15]M. J. Rice and S. Strassler, Solid State Commun. 13, 1389 (1973).

[16]J. J. Ritsko, E. J. Mele, A. J. Heeger, A. G. Mac-Diarmid, and M. Ozaki, Phys. Rev. Lett. 44, 1351 (1980).

[17]H. Shirakawa, T. Ito, and S. Ikeda, Polym. J. 4, 460 (1973); S. Lefrant, L. S. Lichtman, H. Temkin, D. B. Fitchen, D. C. Miller, G. E. Whitewell, and J. M. Burlitch, Solid State Commun. 29, 1919 (1979).

[18]For example, F. Inagaki, M. Tasumi, and T. Miyazawa, J. Raman Spectrosc. 3, 335 (1975).

[19]E. J. Mele and M. J. Rice, Solid State Commun. 34, 339 (1980).

[20]J. Bart and C. H. MacGillvary, Acta Crystallogr. Sect. B 24, 1569 (1968).